14 June 1985, Volume 228, Number 4705 SCIENCE

Tunable Coherent X-rays

David Attwood, Klaus Halbach, Kwang-Je Kim

Summary. A modern 1- to 2-billion-electron-volt synchrotron radiation facility (based on high-brightness electron beams and magnetic undulators) would generate coherent (laser-like) soft x-rays of wavelengths as short as 10 angstroms. The radiation would also be broadly tunable and subject to full polarization control. Radiation with these properties could be used for phase- and element-sensitive microprobing of biological assemblies and material interfaces as well as research on the production of electronic microstructures with features smaller than 1000 angstroms. These short wavelength capabilities, which extend to the K-absorption edges of carbon, nitrogen, and oxygen, are neither available nor projected for laboratory XUV lasers. Higher energy storage rings (5 to 6 billion electron volts) would generate significantly less coherent radiation and would be further compromised by additional x-ray thermal loading of optical components.

The spectral region referred to as the XUV includes soft x-rays and ultraviolet radiation. Photon energies in this region extend from several electron volts (eV) to several thousand electron volts (keV). The primary atomic resonances of elements such as carbon, oxygen, nitrogen, and sodium, as well as resonances from many molecular transitions, appear in this region. In addition, the photon wavelengths in this region match important spatial scales such as the pitch and diameter of biochemical helices, the microstructural features of materials, and the dimensions of the next generation of electronic microcircuits.

The XUV spectral region has not been exploited to the degree warranted by these spectral and spatial features. In many ways it is a difficult region in which to perform experiments. Present XUV radiation sources are far more limited in intensity, tunability, and directionality than lasers, masers, and klystrons, which emit radiation of longer wavelengths. Optical techniques, including reflection, dispersion, and imaging, suffer from photoelectric absorptive effects in this region. Between the wavelengths of about 10 and 1000 angstroms (Å) there are no materials that are both transmissive and capable of supporting an atmosphere of pressure over macroscopic dimensions.

Substantial progress in the development of x-ray optical techniques has been made recently (*1–6*), largely as the result of the need for ever smaller microfabrication capabilities in the electronics industry, research on x-ray emitting, hot dense plasmas for nuclear fusion, and studies of interface formation in materials. For instance, imaging has been demonstrated with normal-incidence x-ray mirrors made with multilayer interference coatings (*1*). X-ray microscopes with diffractive Fresnel zone-plate lenses have produced element-sensitive images of biological systems, in some cases resolved to better than 1000 Å (*2, 8*). X-ray recording instruments with picosecond resolution, initially developed to study energy transport in hot dense plasmas (*9*), are now commercially available.

In order to extend scientific and technological opportunities, a bright source of tunable, partially coherent, XUV radiation is needed. Coherence, in the limited sense used here, refers to the ability to form interference patterns when wave fronts are separated and recombined. Partially coherent radiation is capable of producing clear interference patterns (fringes), but only within limited transverse or longitudinal displacement (*10*). The longitudinal displacement within which fringes can be formed is called the coherence length ℓ_c (*11*), which is given by the wavelength λ times the number of waves of coherence $\lambda/\Delta\lambda$ (spectral purity): $\ell_c = \lambda^2/\Delta\lambda$.

For experiments that utilize phase-sensitive techniques, such as x-ray interferometry and x-ray microholography, a radiation field with full spatial coherence and several micrometers (μm) of longitudinal coherence is often satisfactory. This corresponds to only a few hundred waves of coherence at a wavelength of 100 Å. Radiation with these properties is now attainable as a result of advances in accelerator physics and the development of permanent magnet undulators, structures that produce periodic magnetic fields. In the undulator a narrow beam of relativistic electrons, typically 200 μm in diameter and 50 microradians (μrad) in angular spread, interacts with periodic magnetic fields of precise phase variation to produce directed, tunable radiation, which has narrow spectral features and is nearly diffraction limited, at wavelengths throughout the XUV region (*12*).

Coherence Properties of Radiation from an Undulator

The interaction between an electron beam and a magnetic undulator is illustrated in Fig. 1. A narrowly confined beam of relativistic electrons (or positrons) with an energy equal to γ times the electron rest energy passes between magnets of alternating polarity in a high fidelity undulator of periodicity λ_u. Ex-

The authors are at the Center for X-ray Optics, Lawrence Berkeley Laboratory, Berkeley, California 94720

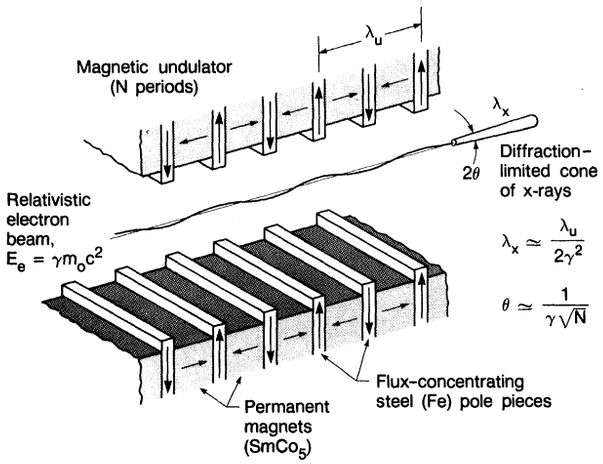

Fig. 1. Partially coherent x-rays are produced when a thin, pencil-like beam of relativistic electrons traverses a periodic magnetic structure. The radiation is relativistically contracted to short wavelengths and condensed to a narrow forward cone.

periencing periodic vertical magnetic fields, the charged particles undergo oscillatory motion in the horizontal plane with the period of oscillation equal to λ_u. Oscillating charges moving at relativistic speeds generate synchrotron radiation that is peaked sharply in the forward direction and that is greatly contracted in wavelength (*13–16*). As observed in the forward direction, the radiation wavelength is relativistically contracted from that of the undulator period λ_u to a wavelength λ given, to a first approximation (*17*), by $\lambda \simeq \lambda_u/2\gamma^2$. For a 1-billion-electron-volt (GeV) electron storage ring ($\gamma \simeq 2000$), this effect contracts centimeter-long oscillation periods to x-ray wavelengths. For an undulator of N periods and a suitable electron beam, the half angle of the radiated emission cone is approximately $1/(\gamma\sqrt{N}$ (*18*), typically 50 μrad for a 100-period undulator. The properties of undulator radiation have been described elsewhere (*19–22*). Table 1 lists typical parameters for a soft x-ray undulator in a 1.3-GeV storage ring.

Short wavelengths, sharp spectral features, and narrow radiation cones are well-known features of undulator radiation. Less well known are the coherence properties of undulator radiation (*23*), properties more generally associated with lasers. Coherent radiation can be well controlled. It can be collimated and projected with a small beam width over long distances, accurately pointed, and focused to small areas; and its wave front can be dissected and recombined to form fringe patterns by means of phase-sensitive techniques such as interferometry and holography. The extension of such capabilities to the XUV spectral region could produce scientific opportunities similar to those that resulted from the development of visible lasers.

The coherence properties of radiation can be characterized by the energy spread of the photons, which is described by their spectral purity $\lambda/\Delta\lambda$, and the phase-space volume in which the photons are contained, $(d \cdot \theta)^2$, where d and θ are measures of photon-beam width and divergence, respectively. Spectral purity determines longitudinal coherence in the direction of propagation as shown in Fig. 2. The phase-space volume is the product of an area and a solid angle, which provides a measure of transverse coherence. The product is minimal for sources of full spatial coherence, limited only by the finite radiation wavelength

$$\frac{d}{2} \cdot \theta = \frac{\lambda}{\pi} \tag{1}$$

where, for a Gaussian intensity distribution, $d/2$ is the $1/e^2$ radius and θ is the $1/e^2$ radiation half angle. Radiation described by Eq. 1 is said to be diffraction-limited. Incoherent radiation, from sources such as ordinary light bulbs, has a broad spectral content and emits from a large area into the largest possible solid angle. Fully coherent radiation has a narrow spectral content ($\lambda/\Delta\lambda \sim 10^{-4}$ to 10^{-6}) and a phase-space volume given by Eq. 1. Partially coherent radiation does not fully possess these limiting properties. Its spatial coherence is defined by Eq. 1, but its longitudinal coherence is limited by a spectral purity of $\lambda/\Delta\lambda \simeq 10^2$ to 10^3.

Because of the direct relation between the electron oscillation and the resulting radiation, the energy spread of the electrons should be small, and the phase-space volume containing the electrons should be equal to or smaller than that given by Eq. 1 for the photons. The phase-space area, which is treated separately for the horizontal and vertical transverse beam directions, is called the emittance (*24*),

$$\epsilon_h = \pi\sigma_h\sigma_{h'} \tag{2}$$

where σ_h and $\sigma_{h'}$ are the horizontal $1/\sqrt{e}$ Gaussian beam radius, in meters, and angle measures, in radians, respectively. Equating the phase-space areas for the electron beam and spatially coherent photons, Eqs. 1 and 2, determines the equivalence condition

$$\sigma_h\sigma_{h'} \simeq \frac{\lambda_{eq}}{4\pi} \tag{3}$$

where λ_{eq} is the shortest wavelength for which full spatial coherence is obtained. From the same electron beam, radiation of longer wavelength will have full spatial coherence, but radiation of shorter wavelengths will have reduced coherence because the phase space of the electrons is overly large. The factor of 4 in Eq. 3 accounts for differences in the common measures of Gaussian electron and photon beam distributions; that is, the $1/e^2$ quantities for photon beams and the $1/\sqrt{e}$ quantities for electron beams.

Advances in modern accelerator physics and storage ring technology have provided the capability of reducing emittance by an order of magnitude (*25, 26*). The 1-GeV storage ring now being considered for construction is designed to provide horizontal and vertical emittances of approximately 7×10^{-9} and 7×10^{-10} π$m \cdot$ rad, respectively. Equation 3 shows that these emittance values correspond to full spatial coherence at wavelengths equal to or greater than λ_{eq} values of 90 Å and 900 Å in the vertical and horizontal directions, respectively. To obtain full spatial coherence at shorter than optimum wavelengths it will be necessary to introduce an aperture in the photon beam. While transmitting only spatially coherent radiation, the aperture will reduce the photon flux by a factor $\lambda^2/\lambda_{eq,v}\lambda_{eq,h}$, where v corresponds to vertical and h to horizontal.

Longitudinal coherence (Fig. 2) provides a measure of permissible separation of wave fronts in the direction of propagation. With wave-front separations less than the coherence length $\ell_c = \lambda^2/\Delta\lambda$, the relation between the phases is maintained, and it is possible to observe clear constructive and destructive interference patterns (fringes). For an electron beam traversing an undulator of finite length, the radiation emitted is that of a harmonic oscillator of N cycles (Fig. 1). The radiation thus occurs in a narrow spectral line of width $\lambda/\Delta\lambda \simeq N$. In the case of relatively strong undulator motion, $K \geq 1$ (*17*), the harmonic content of the electron motion, and thus harmonic content of the radiation, becomes important. In this case the radiation appears in a series of narrow harmonics, each of spectral purity $\lambda/$

$\Delta\lambda \simeq nN$, where n is the harmonic order ($n = 1, 2, 3 \ldots$). Consequently, the observed radiation has a longitudinal coherence length given by

$$\ell_c = \frac{\lambda^2}{\Delta\lambda} \simeq nN\lambda \qquad (4)$$

which is essentially the relativistically contracted length of the undulator.

For the 1-GeV storage ring presently under consideration, Eq. 4 and the parameters in Table 1 indicate a coherence length of approximately 1 μm. Such a coherence length is sufficient for many x-ray microprobing experiments. If additional coherence length is required, or if greater spectral resolution is desired, a monochromator could be employed. With photon beams of such narrow angular content and spatial distribution, spectral resolutions $\lambda/\Delta\lambda$ approaching 10^4 could be anticipated (*27, 28*); however, there would be a concomitant loss in power. With several thousand coherent waves at the exit of a monochromator, longitudinal coherence lengths measured in tens of micrometers could be anticipated. Such long coherence lengths would provide the capability for x-ray holographic microscopy with a relatively deep depth of field.

It is now possible to define a coherent power as that portion of the radiated power residing within a phase-space volume defined by full spatial coherence (Eq. 1) and a desired coherence length. The proposed 1-GeV undulators are expected to radiate with a coherence length of about 1 μm. For experiments in which 1 μm is sufficient, undulator radiation will be fully coherent at wavelengths longer than those determined by Eq. 3. For shorter wavelengths the coherent power decreases according to the relation

$$P_{coh} \propto \frac{I\lambda^2}{\epsilon_h\epsilon_v} \cdot N\lambda \qquad (5)$$

where I is the current and where we have assumed that the total generated power is fixed. For fixed emittance and undulator conditions, increased beam energy (γ) allows the reduction of λ, but imposes a reduction in spatial coherence by a factor of λ^2 and a reduction in longitudinal coherence by a factor $N\lambda$; thus as λ decreases, the coherent power decreases by a factor of λ^3. We will see that from a next generation 1-GeV storage ring we can anticipate an average coherent power of several hundred milliwatts (mW) in the ultraviolet region, which decreases to about 10 mW in the vicinity of the carbon, oxygen, and nitrogen K-absorption edges (20 to 50 Å) and thereafter drops by a factor of λ^3 with further reductions in wavelength.

Coherent X-rays from Low-Emittance Storage Rings

In a description of the characteristics of future undulator radiation sources, the specific properties of a fully designed and optimized facility should be considered so that secondary and non-ideal effects are accounted for. The Advanced Light Source (ALS) proposed by Lawrence Berkeley Laboratory is specifically designed to generate synchrotron radiation, and therefore it includes all features required to achieve the lowest possible emittances plus 12 long, straight sections for magnetic undulators and wigglers (*29*). The storage ring is designed to operate at a beam energy of 1.3 GeV and an average beam current of 400 milliamperes and, specifically, to provide high spectral brilliance and high coherent power in the XUV region. The horizontal emittance from the source is projected to be 7×10^{-9} πm · rad; in one mode of operation the source would incorporate 250 circulating electron bunches of nominally 20-psec duration each.

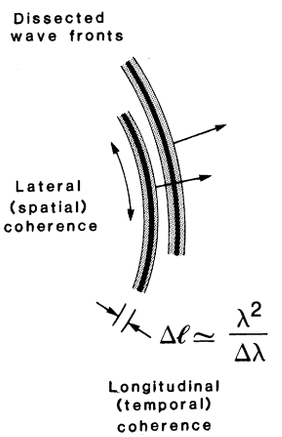

Fig. 2. Partially coherent radiation is described as having full lateral coherence but limited longitudinal (direction of propagation) coherence. Radiation from a single source that has been dissected into wave fronts is shown. After traveling separate paths, perhaps through a sample, the wave fronts will be reunited to form an interference (fringe) pattern. To successfully form an interference pattern, the wave fronts must overlap within a longitudinal coherence length, $\Delta\ell$. For fringe formation to be insensitive to lateral displacement, the radiation should be of full spatial coherence.

The ALS would include four undulators, each designed for a different spectral region. Undulator U_D is specifically designed to cover the spectral range from approximately 200 eV to several keV. This undulator would have 142 periods with a spatial periodicity of 3.5 cm and a peak vertical magnetic field of 0.57 Tesla. The frequency content and spatial distribution of the third-harmonic ($n = 3$) radiation from U_D are shown in Fig. 3. The various spectral peaks would be tuned by varying the magnet gap (*17*), thus varying the effective transit time and temporal frequency. In Fig. 3b, the coherent nature of the radiation is illustrated by the spatial interference pattern of 500 eV (25 Å) radiation at a distance of 10 m from the source. Emanating from the magnetic interaction region, a flux of approximately 10^{16} photons per second radiates into a central cone of 40 μrad by 100 μrad full angle (2θ) from a source area of about 160 μm by 400 μm. The spectral bandwidth is approximately 1 percent. As described in the previous section, the radiated power will be of high spectral brilliance and also largely coherent in nature.

The coherent power considerations for the various undulators are summarized in Fig. 4. Time-averaged coherent power is specifically defined here as that portion of the radiation being of full spatial coherence and having a longitudinal coherence of 1 μm. The vacuum ultraviolet (VUV) undulators (U_A, U_B, and U_C) are each expected to emit radiation with an average coherent power of about 200 mW. For wavelengths shorter than about 100 Å the coherent power falls approximately by a factor of λ^3, as discussed in the previous section. Figure 4 shows that

Table 1. Typical parameters for a soft x-ray undulator.

Parameter	Value
Electron beam energy	1.3 GeV ($\gamma = E/m_oc^2 \simeq 2500$)
Beam current	0.4 amps
Magnetic wavelength (λ_u)	3.5 cm
Magnetic periods (N)	150
Photon wavelength (λ)	$\lambda_u/2\gamma^2 \simeq 30$ Å (400 eV) (Broadly tunable from 100 eV to a few keV)
Bandwidth ($\lambda/\Delta\lambda$)	$N = 150$
Angular divergence (θ)	$1/(\gamma\sqrt{N}) \approx 30$ μrad
Polarization	Linear, circular, and so forth
Temporal structure	20 psec bursts at 500-MHz repetition rate
Coherent power	10 mW at 500 eV, tunable, polarized (spatially coherent; $\ell_c = \lambda^2/\Delta\lambda \sim 1\mu$m)

the 25-Å operating point described spatially and spectrally in Fig. 3 would emit radiation with an average coherent power of 10 mW. This radiation would occur in nominally 20-psec bursts at a 500-megahertz (MHz) repetition rate. At present the greatest flux of coherent soft x-rays is available from a bend magnet (U-15) at Brookhaven's National Synchrotron Light Source (NSLS), as indicated in Fig. 4. When the soft x-ray undulator (X-1) becomes available at NSLS, the coherent power available at that facility should rise by three orders of magnitude. For comparative purposes, Fig. 4 also shows the domain of present atomic and molecular lasers (the shaded region extending to about 1000 Å) (*30*) as well as recent nonlinear laser-harmonic and mixing techniques (*31–34*). The nonlinear mixing techniques are capable of producing radiation at wavelengths less than 1000 Å, but the radiated power declines rapidly, typically as a function of the wavelength raised to an exponent of the order of the nonlinearity involved, for example λ^7 or λ^9.

Recently, researchers at the Lawrence Livermore National Laboratory (LLNL) extended the short-wavelength limit of lasers to the 200-Å region (*35*). In those experiments population inversions were created in plasmas of neon-like selenium and yttrium, which led to single-pass amplified spontaneous emission at several wavelengths. Lines at 206 and 209 Å demonstrated exponential growth in proportion to the length of the gain medium. The lasing medium was a plasma of highly stripped atoms produced with 2-terawatt visible-light pulses from the Novette laser, which was originally built for fusion research. The experiments were guided by a well-characterized set of x-ray spectroscopic and plasma diagnostics and a computational capability that tracked not only the relevant atomic physics but also plasma dynamics and x-ray refractive effects. The peak power in the selenium laser experiments was approximately 400 W in nominally 400-psec pulses. The spectral line widths, dominated by Doppler broadening, were estimated to be of the order of $\lambda/\Delta\lambda \simeq 10^4$, which corresponds to a longitudinal coherence length of about 200 μm. The radiation, however, exceeded the diffraction limits (Eq. 1) by a factor of 50 to 100 in both the horizontal and vertical directions and, thus, was spatially incoherent. The peak power of the spatially coherent radiation derived from this source, that which could be collimated and projected as a thin beam over long distances or focused to diffraction-limited small areas, was of the order of 100 mW.

The large transverse phase space of this class of XUV laser is attributable to the high thermal state of the lasing medium, a rapidly expanding plasma of 1-keV electron temperature. Future experiments are likely to explore the limitations of expanding the plasma as well as the possibility of improving the spatial coherence through the use of transverse mode-selecting techniques. Further experimentation with selenium and yttrium is expected to result in saturated lasing at peak powers three to four orders of magnitude greater than those recorded to date; additional elements and alternate pumping schemes are expected to extend those capabilities to wavelengths somewhat shorter than 100 Å (*36*). Other approaches to XUV lasing, based on the creation of metastable excited states of cold neutral atoms, may also generate laser radiation in the 200-Å region, perhaps of narrower spectral line width and perhaps from significantly smaller facilities (*37*).

In light of these new developments and anticipated progress in XUV lasers, we will review here the capabilities of undulators, to determine how they complement atomic lasers and to consider their own future development. Undulators are expected to produce coherent radiation at wavelengths as short as 10 Å, which would include the absorption edges of elements important to the biological sciences, the physical sciences, and technology, as noted previously (Fig. 4). The coherent radiation typically will have a peak power of 200 W at 200 Å and 10 W at 25 Å and will be generated in nominally 20-psec pulses at megahertz repetition rates. The radiation will be broadly tunable: it will be possible to generate coherent radiation at and near the wavelength of any resonance feature in the soft x-ray or VUV regions. Undulator radiation is naturally polarized; with colinear undulators of orthogonal orientation it will be possible to generate linear, circular or elliptical polarization.

A natural extension of the undulator is the free electron laser (FEL), which for short wavelengths ($\lambda < 1000$ Å) will also be based on the technologies of low-emittance storage rings and periodic magnetic structures (*38*). The extension from undulators to FEL's requires a

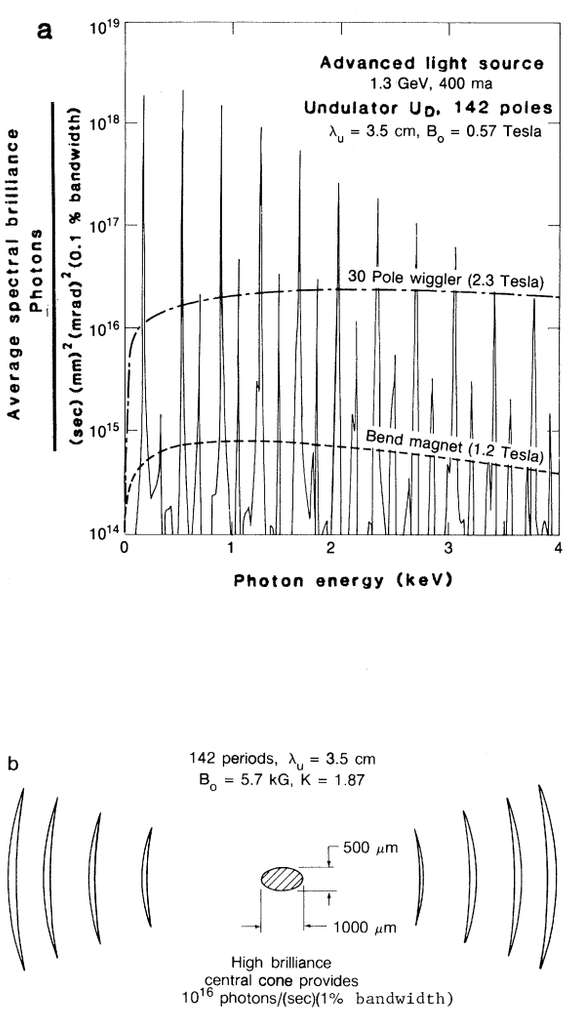

Fig. 3. (a) The frequency structure of undulator radiation consists of sharp spectral peaks of width $1/N$, where N is the number of undulator periods in the magnetic structure. (b) Spatial structure of the third harmonic at a distance of 10 m from the source is shown. Of particular interest is the central radiation cone, which has high spectral brilliance and substantial coherence properties. The characteristics of the photon beam at the source are indicated in the lower left corner.

strong coupling between the generated fields and the driving electron beam. With sufficiently intense fields and appropriate particle dynamics, a density modulation (bunching) could potentially be achieved throughout much of the electron beam. Phase-coherent bunching, extending for as many as several million periods, could then lead to fully coherent radiation of both high peak power (~100 MW) and high spectral purity (*39*) and in which the relative bandwidth $\lambda/\Delta\lambda$ would be proportional to the number of electron modulation periods (of the order of 10^6) rather than the number of undulator periods (of the order of 10^2). Free-electron lasing is now well established in the longer wavelength microwave through visible spectral regions (*40–43*). There are two possible ways to extend FEL techniques to the XUV region, neither of which has yet been pursued in the laboratory because of the lack of appropriate 1-GeV storage ring facilities. One technique, mirror-feedback FEL's, would achieve field intensification through cavity-forming end mirrors, which presently do not exist at sufficiently high reflectivity (*44*). The other approach would make use of very long undulators (N of the order of 10^3) in a storage ring specially built so that intense fields would be generated in a single-pass FEL (*39, 45*). Both of these techniques would provide a natural extension to the coherence properties obtainable with straightforward undulators. Thus storage ring–based technologies are likely to play an important role for many years in the development of coherent radiation of ever shorter wavelength (*46, 47*).

Undulators for the XUV Region

Undulator U_D, designed for use in the proposed 1.3-GeV ALS (*29*), is typical of the type of magnetic structure that would be used for the production of coherent XUV radiation. Designed as a hybrid undulator, it would use samarium cobalt (SmCo) as the flux-generating active magnetic material and soft iron as the field-guiding passive material. The field distribution in the region passed by the electrons is essentially determined by the iron, whereas the field strength is controlled by the active material and the gap distance. Permanent magnet structures of this type (Fig. 1) have been built and operated as x-ray generating devices (*49*).

Permanent-magnet structures are used in this type of application because they offer advantages when critical dimensions such as period and gap are small. The alternate method is to use conventional electromagnets, in which current densities, and thus ohmic heating, are inversely proportional to the linear dimensions of the magnets such that, at some small dimension, cooling becomes an insurmountable task.

When active-material blocks (SmCo) are placed in the structure according to their measured magnetic properties, periodic fields are produced within fairly strict tolerances. Fine tuning of the peak fields is accomplished with tuning studs. The ability to generate on-axis fields within strict tolerances is particularly important for the generation of harmonic radiation, since poor field quality would cause dephasing effects that would result in loss of coherence (*50*).

While it is not expected that improvements in permanent-magnet technology will improve the performance of undulators by very large factors in the foreseeable future, modest improvements can be expected. For example, the production of a new material, whose main ingredients are neodymium and iron, was announced in 1983. This material has magnetic properties (*50*) that will permit given field strengths to be achieved with larger ratios of gap to period than with present materials. With gaps fixed by electron beam considerations, the material will allow magnetic structures to be built with shorter periods, permitting the generation of radiation with proportionately shorter wavelengths.

Microprobing Techniques with Coherent X-rays

The availability of a tunable source of coherent soft x-rays, combined with recent developments in x-ray optical techniques (*3*), should make it possible to construct an x-ray microprobe of sufficient intensity to permit fundamentally new, phase-sensitive experimentation in a number of scientific and technological fields. Various imaging and scattering techniques would be enhanced by the greatly increased photon flux available to study small samples together with the capability of tuning the radiation to the wavelength of interest. For example, with soft x-rays well matched to the absorption edges of elements such as carbon (284), nitrogen (400), and oxygen (532) as well as other elements of relatively low atomic number, such as sodium, phosphorus, sulfur, potassium, and calcium, it should be possible to study elemental distributions and motion within biological specimens without the need for dehydration, fixing, or staining (*52*). Three-dimensional imaging, made possible by combining partially coherent undulator radiation and x-ray microholographic techniques, would complement the information available from electron microscopes of high spatial resolution. Additional techniques, based on polarization control (*53*), could permit further investigation of biochemical assemblies in which image contrast, or scattering, would be enhanced by the resonance

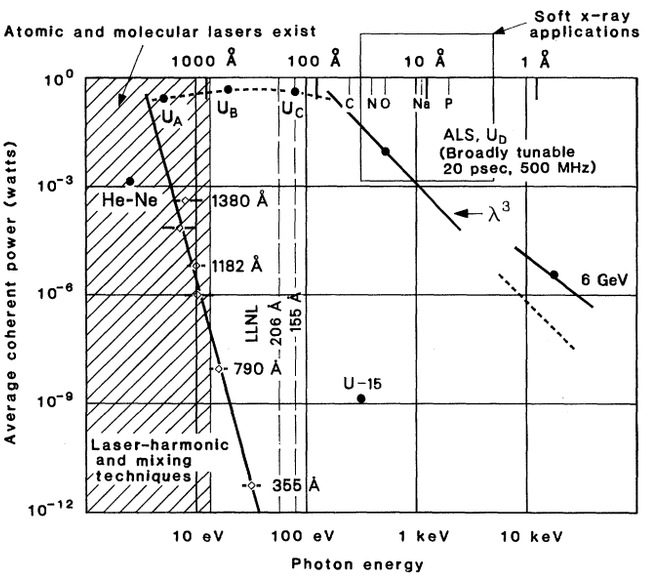

Fig. 4. Broadly tunable coherent power is achievable, in the soft x-ray region, with long magnetic undulators in a specially designed low-emittance storage ring. Undulators U_A, U_B, and U_C provide continuous coverage throughout the vacuum ultraviolet region. Undulator U_D of the ALS would provide continuous coverage through the soft x-ray region. U-15 denotes a bending magnet source at NSLS. The shaded area to the left shows the domain of atomic and molecular lasers, which is constrained primarily to wavelengths of about 1000 Å and longer. Recent laser results at 206 Å and 155 Å driven by the Novette laser at LLNL are indicated. The range of radiation produced by laser-harmonic and mixing techniques is also shown. In the soft x-ray spectral region, which includes the important K-absorption edges of carbon, nitrogen, and oxygen, only undulators could provide significant coherent power in the near term. Coherent power is defined here as radiation having full spatial coherence and a longitudinal coherence length of 1 μm.

between XUV wavelength, polarization rotation, and structural features such as helical pitch, diameter, and conformational details (*54*). Figure 5 illustrates how linear, circular, and elliptical polarization could be obtained with a pair of colinear undulators of orthogonal orientation.

The microprobing of small samples with coherent x-rays would permit studies with spatial and temporal resolutions of the order of hundreds of angstroms and tens of picoseconds (generally in some inverse relation) and would bring new capabilities to many scientific fields. In the fields of atomic and molecular physics (*55*), it would be possible to obtain new insights into many-electron phenomena and other aspects of atomic structure and dynamics, including threshold resonances. Characterization of initial and final atomic states would become even more precise with the capability of studying microscopic gas samples with tunable, high-flux photon beams. In the field of materials science, these same capabilities would permit new studies of atomic order in thin films, of interface formation, and of surfaces, to name a few areas (*56*). Chemists studying photoexcitation and photoionization (*57*) at XUV wavelengths would benefit from a significant extension of capabilities. High-brilliance radiation, combined with appropriate focusing optics, could permit the concentration of unprecedented flux (in excess of 10^{13} photons per second within a spectral width $\Delta\lambda/\lambda$ approaching 10^{-4}) onto microscopic samples. The resultant interaction products could be studied with high spatial, temporal, and spectral resolution by matching instrumentation to the new high-brilliance source. In fact, researchers in this field have already demonstrated the ability to selectively fragment molecular bonds and, as a consequence, "foresee the use of tunable soft x-rays as scalpel-like tools to break large organic molecules around certain selectable atoms (C, N, or O) within the molecule" (*58*). As a last example, industrial scientists would have a new tool for optimizing photoresist materials for x-ray lithographic recording and subsequent replication of microstructures with features smaller than 1000 Å (*59*).

A diagram of a coherent x-ray microprobe driven by undulator radiation is shown in Fig. 6. Partially coherent radiation, generated within the undulator by a nominally 1-GeV electron beam (not shown), would propagate to the right. A

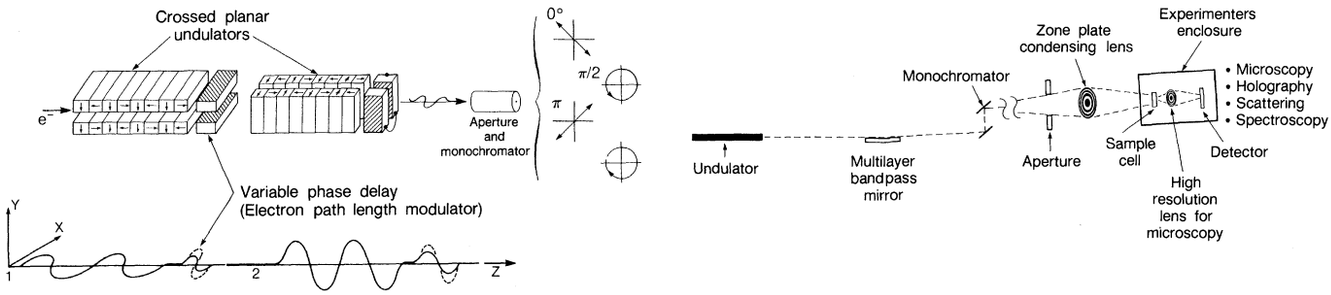

Fig. 5 (left). Arbitrarily polarized radiation, including linear, circular, and elliptical polarization, can be achieved with a pair of colinear undulators of orthogonal orientation. The electron pathlength in the intermediate region controls the phase relation between the radiation from the two undulators and thus determines the resultant polarization state. Fig. 6 (right). A generalized soft x-ray microprobe is diagramed. There is a difference in scale after the monochromator. Such a capability will bring new scientific opportunities to the biological and physical sciences from such techniques as x-ray and vacuum-ultraviolet microscopy, microholography, scattering, and spectroscopy.

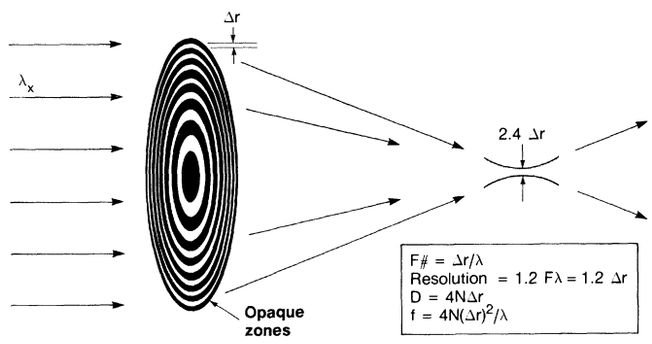

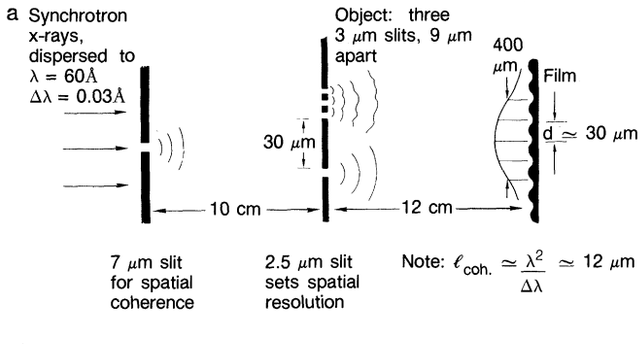

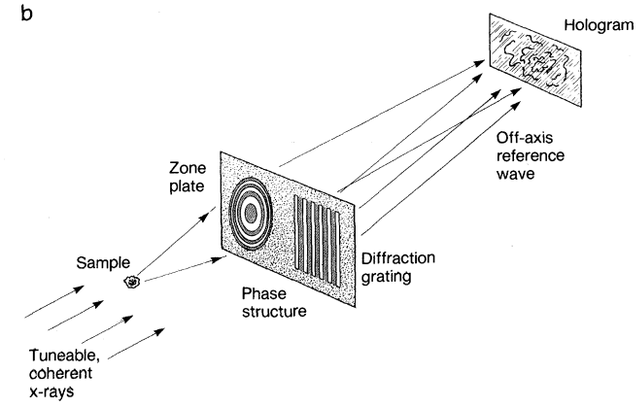

Fig. 7 (left). Diffractive focusing of soft x-rays with a Fresnel zone plate is illustrated. With an outer zone width of Δr (perhaps 500 to 1000 Å), a focal region waist of $2.4\Delta r$ is achieved. The equivalent lens $F\#$, imaging resolution, diameter, and focal length are indicated. The use of more familiar refractive lenses, those commonly used for visible light, is precluded by absorptive effects in the x-ray region. Fig. 8 (right). (a) Diagram of an experiment by Aoki and Kikuta that demonstrated off-axis x-ray holography with synchrotron radiation (*66*). (b) A possible extension of x-ray microholography is shown. With modern x-ray optical techniques and additional coherent power by a factor of 10^9, the experiments in (a) could be redesigned and repeated with significantly improved spatial and temporal resolution, perhaps of the order of 1000 Å and 1 millisecond, at soft x-ray wavelengths.

multilayer interference mirror may be desirable for harmonic selection (Fig. 3a) and modest spectral definition (*7*), $\lambda/\Delta\lambda \simeq 30$ to 100. A circular collimator would generally be used to remove angular structure outside the central radiation cone (Fig. 3b). A monochromator is shown for those experiments that would benefit from improved spectral resolution or longer coherence length. The monochromator would be followed by a Fresnel zone plate, a circular microstructure that would serve as a focusing or condensing lens, depending on the application. The zone-plate lens would be followed by an experimenter's enclosure that would include the sample under study and whatever additional components would be required for the particular technique employed, for instance, microscopy, microholography, scattering, or spectroscopy. Each of these techniques has its own requirements and therefore would not benefit from all the components indicated in Fig. 6.

Focusing by a Fresnel zone plate is accomplished by diffraction from a circular pattern of alternating opaque and transmissive zones (Fig. 7). Although properly understood as constructive interference of radiation scattering from regions whose pathlengths to the focal region differ by integral values of the wavelength, the focusing can be readily understood in terms of diffraction from a circular grating pattern whose spatial period varies from very large values ($d >> \lambda$) near the axis to values approaching the radiation wavelength near the periphery. Since the spatial period is relatively short in the outer regions of a zone plate, large diffraction angles, $\theta \simeq \lambda/\Delta r$, result. Nearer the axis of symmetry the radiation is scattered by a structure of longer spatial period; therefore, smaller diffraction angles result. Opaque structures, which diffract about 10 percent of the incident radiation into the first-order real focus, have been fabricated by several groups. An excellent example, which would serve well as the microprobe condenser lens in Fig. 5, is the 500-zone, freestanding, gold structure, with an outer diameter of 640 μm and an outer zone width of 3200 Å, fabricated by D. Shaver and his colleagues at the Massachusetts Institute of Technology and LLNL (*60*). High-resolution zone plates, with outer zones of 600 Å to 700 Å, have been fabricated by groups at Göttingen (*61*) and IBM (*62*). The highest resolution biological images based on zone-plate microscopy, obtained by Schmahl, Rudolph and Niemann (*8*), clearly demonstrate the capabilities of zone plates as imaging elements for soft x-rays. Phase plates, a form of zone plate in which the alternate opaque zones are replaced by transmissive materials, could eventually provide important improvements in diffraction efficiency, to values approaching 40 percent in the first-order focus (*63–65*).

The application of coherent techniques to the x-ray region would be, in some sense, a major undertaking; but in fact some of the work has already been done, and we can speculate somewhat about the not too distant future. As an example, consider x-ray holography. In Fig. 8a we describe one in a series of pioneering x-ray holographic experiments performed in the early 1970's by Aoki, Kikuta, and their colleagues (*66*). Synchrotron x-rays were dispersed with a monochromator to give $\Delta\lambda/\lambda \simeq 5 \times 10^{-4}$, which corresponds to a coherence length of 12 μm at a wavelength of 60 Å. Spatial coherence was obtained, at a considerable cost in available flux, by introducing a 7-μm slit, as shown in the mask to the left of Fig. 8a. The emerging radiation then diffracted outward, illuminating a second mask that contained the "object" (three slits) and a narrow slit that generated an off-axis reference wave. The two emerging wave fronts overlapped at the film plane, forming an interference pattern. The experimental geometry was arranged to produce an interference pattern of sufficiently long average period (~30 μm) to permit visible light (He-Ne laser) image reconstruction, a technique that takes advantage of the capacity of the human eye and brain in combination to recognize pattern formations. The exposure time of these early experiments was approximately 1 hour. Many scientists will have no difficulty understanding this work in terms of a Young's double-slit interference experiment, in which the second slit (the "object") has structure. The Japanese group performed other x-ray holographic experiments during the same period, some with the Gabor in-line geometry, in which images of chemical fibers and red blood cells were recorded and reconstructed (*66*).

An extension of these x-ray holographic techniques is suggested by Fig. 8b, in which the availability of coherent undulator radiation is assumed as well as advancements in the fabrication of diffractive x-ray optical components. A small sample, perhaps an assemblage of three-dimensional biological structures, could be probed by partially coherent x-rays. A phase plate, consisting of a Fresnel lens and a diffraction grating, could serve the dual purpose of capturing the diffracted wave from the object and generating an off-axis reference wave. The two waves would overlap in a limited area of a holographic recording material and form a complex interference pattern with the carrier frequency (average period) set by the wavelength and intersection angles. This is a conventional view of holographic microscopy (*67, 68*), in which high-resolution features are captured by a microscope objective lens of high numerical aperture, extrapolated to the soft x-ray region of the spectrum. Except for the enhancement of diffraction efficiency by a factor of 4, which would be gained by the use of a phase structure, all the requisite technologies have been demonstrated. If a facility like the proposed ALS were available, where coherent power would be enhanced by a factor of 10^9 beyond that available for the experiment described in Fig. 8a, these experiments could be performed with significantly improved spatial and temporal resolution, perhaps of the order of 1000 Å and 1 millisecond. A survey of relevant x-ray holographic techniques, along with the results of recent in-line interference experiments at Brookhaven, is presented in a recent article by Howells, who also points to the promise of undulators as coherent-radiation sources (*69*). The coherence requirements for the study of several specific biological specimens have been discussed by Solem and Chapline (*70*).

Conclusion

A clear path to experimentation with phase-coherent x-rays has been described. Based on well-developed accelerator and magnetic-undulator technologies, partially coherent radiation, tunable from the vacuum ultraviolet to the soft x-ray spectral regions, could be made available within a few years with a next generation 1-GeV storage ring. The optical techniques needed to exploit that region have already been demonstrated and continue to be improved. Phase-sensitive techniques, previously available only at longer wavelengths (visible, infrared, microwave, and so on), would become available for x-rays. With diffraction-limited sources of even modest temporal coherence, unprecedented control of this radiation would be at hand. High photon fluxes, directed toward diffraction-limited sample volumes in picosecond pulses, could open new opportunities in studies of photochemical processes, atomic and molecular transitions, material interfaces, and biological structures. It would be presumptuous to attempt a prediction of the specific fields

that would provide the most valued breakthroughs (*71*).

Undulator-based facilities would permit demonstration experiments, provide breakthrough scientific opportunities, and provide an exciting environment that would attract scientists and students alike. Because of cost constraints, a next generation 1-GeV facility would necessarily be a project shared by the various scientific disciplines. Additional progress toward obtaining fully coherent radiation will take place as short-wavelength free-electron lasers, based on these same storage ring and magnetic undulator technologies, evolve in the coming years (*72*).

References and Notes

1. D. T. Attwood and B. L. Henke, Eds., *AIP Conference Proceedings* (American Institute of Physics, New York, 1981), vol. 75.
2. G. Schmahl and D. Rudolph, Eds., *X-Ray Microscopy* (Springer-Verlag, Berlin, 1984).
3. J. H. Underwood and D. T. Attwood, *Phys. Today* **37**, 44 (April 1984).
4. D. T. Attwood *et al.*, *AIP Conf. Proc.* **90**, 254 (1982).
5. E. Spiller, in *Handbook On Synchrotron Radiation*, E-E. Koch, Ed. (Elsevier, New York, 1983), vol. 1B, pp. 1091–1129.
6. J. Kirz and H. Rarback, *Rev. Sci. Instrum.* **56**, 1 (1985).
7. J. H. Underwood and T. W. Barbee, *Nature (London)* **294**, 429 (1981). Also see the articles on multilayers by T. W. Barbee (p. 131) and E. Spiller (p. 124) in (*1*).
8. G. Schmahl, D. Rudolph, B. Niemann, *Ann. N.Y. Acad. Sci.* **342**, 368 (1980); A. L. Robinson, *Science* **215**, 150 (1982); J. M. Kenney *et al.*, *J. Microsc. (Oxford)*, in press.
9. G. L. Stradling *et al.*, *IEEE J. Quantum Electron. QE-19*, 604 (1983).
10. M. Born and E. Wolf, *Principles of Optics* (Pergamon, New York, ed. 6, 1983), chap. 10.
11. R. Collier, C. Burckhardt, L. Lin, *Optical Holography* (Academic Press, New York, 1971), pp. 26–33 and 137–152; M. Born and E. Wolf (*10*), pp. 316–323.
12. K-J. Kim, K. Halbach, D. T. Attwood, *AIP Conf. Proc.* **119**, 267 (1984).
13. J. D. Jackson, *Classical Electrodynamics* (Wiley, New York, ed. 2, 1975), pp. 672–679.
14. A. A. Sokolov and I. M. Ternov, *Synchrotron Radiation* (Pergamon, New York, 1968).
15. E-E. Koch, Ed., *Handbook on Synchrotron Radiation* (Elsevier, New York, 1983), vol. 1A, chap. 2.
16. H. Winick *et al.*, *Phys. Today* **34**, 50 (May 1981).
17. A more accurate form of the relativistic contraction formula that accounts for increased transit time due to oscillatory motion in the periodic magnetic field is $\lambda \simeq (\lambda_u/2\gamma^2)[1 + (K^2/2)]$, where the undulator paramater $K = 0.93B_o\lambda_u$, B_o is the peak magnetic field strength in tesla, and λ_u is the undulator period in centimeters. For an undulator, K is typically of the order of unity. The wavelength of undulator radiation is tuned either through mechanical variation of the magnetic gap, and thus variation of $K(B_o)$, or through variation of the electron beam energy γ.
18. The cone of radiation emitted by an electron undergoing a single oscillation is characterized by an angle γ^{-1}. However when the electron undergoes N phase-coherent undulations it is possible for the fields to interfere, which results in a narrowed radiation cone. To observe this effect the undulator must be followed by a monochromator of modest resolution $\lambda/\Delta\lambda \simeq N$. Although this narrowing of the cone follows directly from the electromagnetic formalism (*19–22*), it is useful to consider the following arguments. The diffraction-limited half angle of a distributed electromagnetic source of length L and wavelength λ is given by $\theta \simeq \sqrt{\lambda/L}$ [in (*10*), p. 441; essentially, it is a depth of focus argument for diffraction-limited radiation of half angle $\theta \simeq 1.2\lambda D$ and apparent source size, or waist, $D = L\theta$]. When the undulator length is expressed as $L = N\lambda_u$, and the relativistically contracted wavelength is approximated by $\lambda/\lambda_u \simeq \gamma^{-2}$, the half angle of the emitted radiation is given by $\theta \simeq \lambda/N\lambda_u = 1/(\gamma\sqrt{N})$. A significant feature of modern storage rings is that the collective electron beam is of sufficiently narrow width and divergence that the combined trajectories of the electrons do not obscure these single-electron effects.
19. D. F. Alferov, Y. A. Bashmakov, E. G. Bessonov, *Sov. Phys. Tech. Phys. (Engl. Transl.)* **18**, 1336 (1974); D. F. Alferov *et al.*, *Part. Accel.* **9**, 233 (1979).
20. B. M. Kincaid, *J. Appl. Phys.* **48**, 2684 (1977).
21. S. Krinsky, *IEEE Trans. Nucl. Sci.* **NS-30**, 3078 (1983).
22. A. Hofmann, *Phys. Rep.* **64**, 253 (1980); Stanford Synchrotron Radiation Project Report 77/05, II-49 (Stanford University, Palo Alto, Calif., 1977).
23. A. M. Kondratenko and A. N. Skrinsky, *Opt. Spectrosc. (USSR)* **42**, 189 (1977).
24. Random particle trajectories about a beam can be characterized by their positon x and angle x', in each of the transverse directions. The beam emittance is defined as the area in this x, x' phase space that includes all particles within one standard deviation of the mean. For cases in which this phase-space area is elliptical, with major and minor axes parallel to x and x', the beam emittance is given by $\epsilon_x = \pi\sigma_x\sigma_{x'}$, where σ_x and $\sigma_{x'}$ are the axes values.
25. S. Krinsky, in *Free Electron Generation of Extreme Ultraviolet Coherent Radiation*, J. M. J. Madey and C. Pellegrini, Eds. (American Institute of Physics, New York, 1984), pp. 44–49.
26. H. Wiedemann, *J. Phys. (Paris) Colloq.* **C1** (Supp. 2), 201 (1983).
27. M. R. Howells, *Nucl. Instrum. Meth.* **172**, 123 (1980); *ibid.* **177**, 127 (1980).
28. R. L. Johnson, in *Handbook on Synchrotron Radiation*, E-E. Koch, Ed. (Elsevier, New York, 1983), vol. 1A, pp. 173–260.
29. D. Attwood, B. Hartline, R. Johnson, Eds., *The Advanced Light Source: Scientific Opportunities* (Publication 5111, Lawrence Berkeley Laboratory, University of California, Berkeley, 1984); R. Sah, Ed., Appendix A, *The Advanced Light Source: Technical Design* (Publication 5111, Appendix A, Lawrence Berkeley Laboratory, University of California, Berkeley, 1984).
30. T. Srinivasan *et al.*, in *Laser Spectroscopy VI*, H. P. Weber and W. Luthy, Eds. (Springer-Verlag, Berlin, 1983), pp. 385–386.
31. H. Schomburg, H. F. Döbele, B. Rückle, *Appl. Phys. B.* **30**, 131 (1983).
32. A. H. Kung, *Opt. Lett.* **8**, 24 (1983).
33. T. Srinivasan *et al.*, *IEEE J. Quantum. Electron.* **QE-19**, 1270 (1983).
34. J. Boker, P. H. Bucksbaum and R. R. Freeman, *Opt. Lett.* **8**, 217 (1983).
35. D. L. Matthews *et al.*, *Phys. Rev. Lett.* **54**, 110 (1985); M. D. Rosen *et al.*, *ibid.*, p. 106; A. L. Robinson, *Science* **226**, 821 (1984).
36. N. Ceglio, Ed., *Proceedings of the Symposium on the Applications of Laboratory X-ray Lasers*, Asilomar, Calif., 17–19 February 1985, in preparation.
37. S. E. Harris, *Opt. Lett.* **5**, 1 (1980); S. E. Harris *et al.*, in *Proceedings of the IX International Conference on Atomic Physics*, N. Forston, Ed. (Singapore World Science, Singapore, in press).
38. J. M. J. Madey and C. Pellegrini, Eds., *Free Electron Generation of Extreme Ultraviolet Coherent Radiation* (American Institute of Physics, New York, 1984).
39. J. Murphy and C. Pellegrini, *J. Opt. Soc. Am.* **1B**, 530 (1984).
40. J. M. J. Madey, *J. Appl. Phys.* **42**, 1906 (1971); J. M. J. Madey, M. A. Schwettman, W. M. Fairbank, *IEEE Trans. Nucl. Sci.* **NS-20**, 980 (1973).
41. M. Billardon *et al.*, *Phys. Rev. Lett.* **51**, 1652 (1983).
42. B. E. Newman *et al.*, *J. Opt. Soc. Am.* **1B**, 505 (1984).
43. T. J. Orzechowski *et al.*, in preparation.
44. D. T. Attwood *et al.*, in (*38*), pp. 294–313. T. W. Barbee and his colleagues report recent experiments in which normal incidence reflectances near 60 percent were achieved at a wavelength of 170 Å (private communication).
45. K-J. Kim, Ed., *Coherent X-rays and Vacuum Ultraviolet Radiation from Storage Ring–Based Undulators and Free Electron Lasers* (Publication 18945, Lawrence Berkeley Laboratory, University of California, Berkeley, 1985).
46. N. Bloembergen, *IEEE J. Quantum Electron.* **QE-20**, 556 (1984).
47. A. L. Schawlow, *ibid.*, p. 558.
48. K. Halbach, *J. Phys. (Paris) Colloq.* **C1** (Supp. 2), 211 (1983).
49. E. Hoyer *et al.*, *IEEE Trans. Nucl. Sci.* **NS-30** 3118 (1983).
50. B. Kincaid, *J. Opt. Soc. Am.*, in press.
51. M. Sagawa *et al.*, *J. Appl. Phys.* **55**, 2083 (1984).
52. J. Kirz and D. Sayre, in (*2*), pp. 262–267.
53. K-J. Kim, *Nucl. Instrum. Methods* **219**, 425 (1984).
54. F. Allen and C. Bustamante, Eds., *Applications of Circularly Polarized Radiation* (Plenum, New York, 1985).
55. B. Crasemann and F. Wuilleumier, *Phys. Today* **37**, 1 (June 1984).
56. P. Eisenberger and M. Knotek, Eds., *Planning Study for Advanced National Synchrotron Radiation Facilities* (U.S. Department of Energy, Government Printing Office, Washington, D.C., 1984).
57. G. Pimentel, Ed., *Report of the Committee to Survey the Chemical Sciences* (National Academy of Sciences, Washington, D.C., in press).
58. W. Eberhardt *et al.*, *Phys. Rev. Lett.* **50**, 1038 (1983).
59. A. R. Neurether *et al.*, in *X-Ray Lithography and Applications of Soft X-rays to Technology*, A. D. Wilson, Ed. (Society of Photographic Instrumentation Engineers, Bellingham, Wash., 1984), pp. 64–71.
60. D. C. Shaver *et al.*, *J. Vac. Sci. Technol.* **16**, 1626 (1979); H. I. Smith *et al.*, in (*2*), p. 52 and figure 7.2.
61. G. Schmahl *et al.*, in (*2*), pp. 63–74.
62. M. Hatzakis, C. H. Ting, N. Viswanathen, paper presented at the Sixth International Conference on Electron and Ion Beam Science and Technology, San Francisco, Calif., May 1974; D. Kern *et al.*, in *Science With Soft X-Rays*, F. J. Himpsel and R. W. Klaffky, Eds. (Society of Photographic Instrumentation Engineers, Bellingham, Wash., 1984), pp. 204–213.
63. M. Sussman, *Am. J. Phys.* **28**, 394 (1960).
64. J. Kirz, *J. Opt. Soc. Am.* **64**, 301 (1974).
65. R. O. Tatchyn, P. L. Csonka, I. Lindau, *ibid.* **B1**, 806 (1984).
66. S. Aoki, Y. Ichihara, S. Kikuta, *J. Appl. Phys. (Tokyo)* **11**, 1857 (1972); S. Kikuta *et al.*, *Opt. Commun.* **5**, 86 (1972); S. Aoki and S. Kikuta, *J. Appl. Phys. (Tokyo)* **13**, 1385 (1974).
67. R. F. Van Ligten and H. Ostenberg, *Nature (London)* **211**, 282 (1966).
68. D. T. Attwood *et al.*, *Phys. Rev. Lett.* **40**, 184 (1978).
69. M. Howells, in (*2*), pp. 318–335.
70. J. C. Solem and G. F. Chapline, *Opt. Eng.* **23**, 193 (1984).
71. For a series of papers on the development of lasers and related techniques for the visible and near visible spectral regions, see C. H. Townes, *IEEE J. Quant. Electron* **QE-20**, 547 (1984); W. E. Lamb, *ibid.*, p. 551; N. Bloembergen, *ibid.*, p. 556; A. L. Schawalow, *ibid.*, p. 558; C. N. K. Patel, *ibid.*, p. 561.

72. We thank our colleagues at Lawrence Berkeley Laboratory and elsewhere for their contributions to this article. This work was supported by the Office of Basic Energy Science, U.S. Department of Energy, under contract DE-AC03-76SF-00098.